行政院國家科學委員會專題研究計畫 期中進度報告

類澱粉質纖維分子結構之固態核磁共振研究--纖維蛋白超分子結構之測量(總計畫暨子計畫二)(2/3)
期中進度報告(精簡版)

計 畫 類 別 ： 整合型
計 畫 編 號 ： NSC 95-2627-M-002-002-
執 行 期 間 ： 95 年 08 月 01 日至 96 年 07 月 31 日
執 行 單 位 ： 國立臺灣大學化學系暨研究所

計 畫 主 持 人 ： 陳振中
共 同 主 持 人 ： 陳俊顯

處 理 方 式 ： 期中報告不提供公開查詢

中 華 民 國 96 年 05 月 17 日

行政院國家科學委員會補助專題研究計畫 □ 成 果 報 告 ☑期中進度報告

類澱粉質纖維分子結構之固態核磁共振研究—纖維蛋白超分子結構之測量 (總計畫暨子計畫二)

計畫類別：□ 個別型計畫　　☑ 整合型計畫
計畫編號：NSC 95－2627－M －002－002－
執行期間：　95 年　8 月　1 日至　96 年　7 月　31 日

計畫主持人：陳振中
共同主持人：陳俊顯
計畫參與人員：　李心文、林妮嫻

成果報告類型(依經費核定清單規定繳交)：☑精簡報告　□完整報告

本成果報告包括以下應繳交之附件：
□赴國外出差或研習心得報告一份
□赴大陸地區出差或研習心得報告一份
□出席國際學術會議心得報告及發表之論文各一份
□國際合作研究計畫國外研究報告書一份

處理方式：除產學合作研究計畫、提升產業技術及人才培育研究計畫、列管計畫及下列情形者外，得立即公開查詢
□涉及專利或其他智慧財產權，□一年□二年後可公開查詢

執行單位：國立台灣大學化學系

中　華　民　國　95 年 5　月　17　日

摘要

此計畫是探討類澱粉質纖維的分子結構，計劃的第二年主要為（一）製備並檢測含 ^{13}C 與 ^{15}N 同位素標籤的普里昂纖維；（二）測量並鑑定蛋白纖維中的 ^{13}C 與 ^{15}N 化學位移；（三）測量纖維中β褶板構象的位置與分佈；（四）測量殘基的脊柱扭轉角度。我們集中研究以下的鼠類普里昂蛋白之多肽序列：

Ac-KHVAGAAAAGAVVG

109 122

利用固態多肽合成技術，我們成功於不同殘基位置加入 ^{13}C 與 ^{15}N 的同位素標籤（陳振中、俞聖法），經過核磁共振測量（陳振中），原子力顯影術測量（陳俊顯），分子動力學計算（陸駿逸），目前已建立了此纖維分子的初始結構模型：

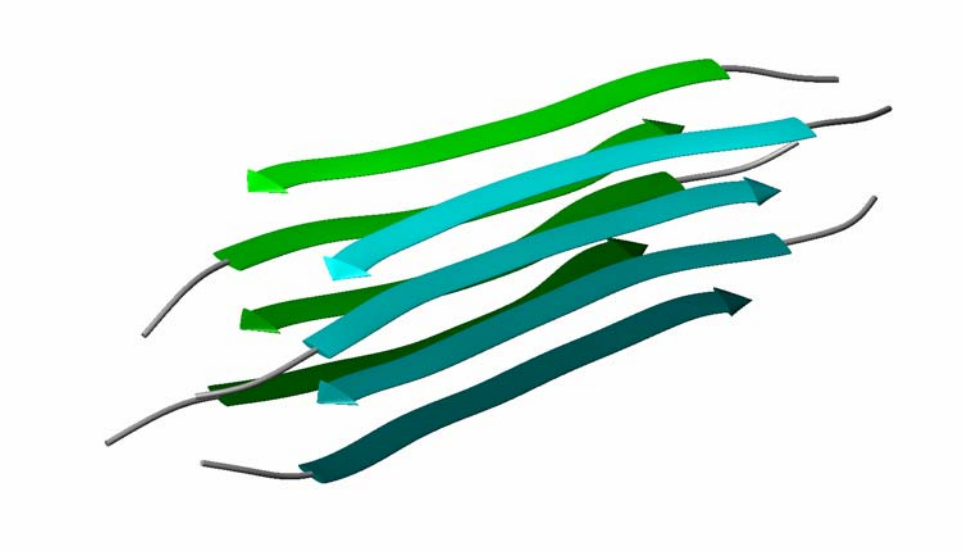

此模型包含兩條纖維分子，纖維分子之間是平行的走向，分子內的β束則是反向平行。文獻上許多報告顯示類澱粉質纖維分子有極強的相互依附特性，我們的結果首次揭露此等依附現象是由殘基支鏈的疏水性及空間位阻效應所產生。

Abstract

The main objective of this interdisciplinary project is to study the molecular structure of the amyloid fibrils formed by the peptide fragment of hamster prion protein. In the second year of this project, there are several specific aims: (i) preparation and characterization of selective ^{13}C and ^{15}N labeled fibrils; (ii) assignment of the ^{13}C and ^{15}N isotropic chemical shifts of the residues; (iii) determination of the β-sheet organization and the hydrogen-bond registry between the neighboring β strands; (iv) determination of the backbone torsion angles. In our study, we focus on the following peptide fragment of the hamster prion protein:

Ac-KHVAGAAAAGAVVG

109 122

Using solid-phase peptide synthesis, we are able to label the fibrils with ^{13}C and ^{15}N isotopes at different residues (Chun-Chung Chan and Sheng-Fa Yu). On the basis of solid-state NMR measurements (Chun-Chung Chan), atomic force microscopic measurements (Chun-Hsien Chen), and molecular dynamics simulations (Chun-Yi Lu), we have constructed a preliminary model for our target fibrils:

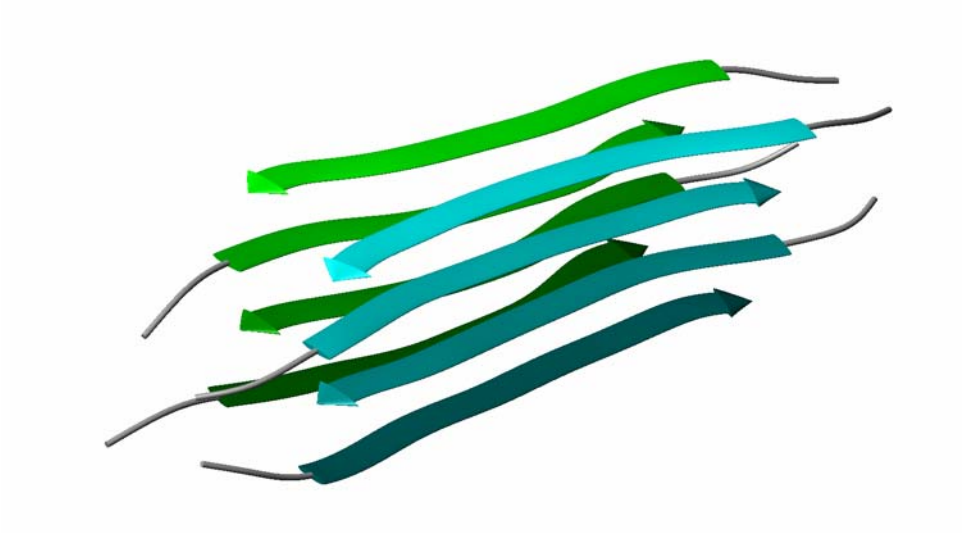

This model comprises two fibrils. The neighboring β-strands within the same fibril molecule have anti-parallel organization, with all the β-strands aligned in such a way that the residues Ala-117 form a linear chain along the fibril axis. On the other hand, the two fibrils are oriented in parallel fashion and are spatially close to one another. In the literature, it is well known that amyloid fibrils have a strong propensity to aggregate. Our data indicate that such lateral association is due to the hydrophobic interaction of the sidechains.

I. Introduction

The main objective of this proposal is to construct a high-resolution structural model for the amyloid fibrils formed by the hamster prion peptide. The class of amyloid fibrils we are targeting in this proposal is associated with prion diseases such as the Creutzfeldt-Jakob disease and the "Mad Cow" disease. In view of the spectacular success of the study of non-crystalline protein structures using solid-state NMR spectroscopy, we propose to use the same spectroscopic method, complemented by a series of other spectroscopic methods and molecular dynamics simulations, to investigate the molecular structures and the fibrillization dynamics of our target fibrils. Our ultimate goal is to unravel the mechanism of prion formation so that appropriate medical treatments can be developed.

We have employed a series of physical techniques to determine the molecular structure of our target fibrils. The atomic force microscopy and solid-state NMR data obtained thus far provide very useful structural constraints for our molecular dynamic simulations, from which we have developed a structural model for our target fibrils.

II. Materials and methods

Sample Preparation and Characterization. All the chemicals were obtained from NovaBiochem unless stated otherwise. $SHPrP_{109–122}$ peptides, with the sequence MKHMAGAAAAGAVV, were synthesized on a PS3 (Rainin) peptide synthesizer, using a Rink amide resin (0.6 mequiv/g substitution level; Novabiochem), 9-fluorenylmethoxycarbonyl (FMOC) chemistry with 2-(1H-benzotriazole-1-yl)-1,1,3,3-tetramethyluronium hexafluorophosphate activation, and acetic anhydride capping in the final step to protect the N-terminus. The synthesis scale was 0.1 mmol, with a 5-fold excess and a 2 h coupling time for each unlabeled amino acid, and a 2-fold excess and a 4 h coupling time for each labeled amino acid. Crude peptides were cleaved from the synthesis resin using standard protocols [reaction for 120 min in 94% trifluoroacetic acid (TFA) with 2.5% ethanedithiol, 2.5% D.I. water and 1% thioanisole scavengers], precipitated in cold *tert*-butyl methyl ether (TBME). Precipitated peptides were washed three times with cold TBME and then lyophilized. The crude material was purified by high-performance liquid chromatography at 50°C, using a water/acetonitrile gradient with 0.1% TFA and a preparative scale Vydac C18 reverse-phase column. Samples of 6 mg per injection were dissolved in 100 μL pure TFA and then diluted to 5 mL with 10% acetonitrile in D.I. water before being injected onto the column. Fractions containing $SHPrP_{109–122}$ were collected at the concentration of 23% acetonitrile and were frozen in liquid nitrogen immediately after being collected. Peptide purity was at least 90% as determined by MALDI-TOF mass spectrometry. The yield of purified peptide, relative to the 0.1 mmol synthesis scale, was approximately 25%. Samples for solid-state NMR measurements were isotopically labeled at selected positions as summarized in Table 1. ^{13}C- and ^{15}N-labeled amino acids with FMOC protection were obtained from Cambridge Isotope Laboratories, CortecNet and Isotec. Fibril samples were formed by dissolution of purified $SHPrP_{109–122}$ at a peptide concentration of 745 μM in 100 mM NaCl and 20 mM N-Cyclohexyl-2-aminoethanesulfonic acid (HEPES buffer, pH 7.4), with addition of 0.01% NaN_3. Dissolution was assisted by sonication. Fibrils formed after incubation at 37°C for one day, appearing as a visible precipitate. For SSNMR measurements, the salts were subsequently removed by repeated dissolution in D.I. water and centrifuge for three times, and then lyophilized.

Tapping Mode Atomic Force Microscopy. Tapping mode atomic force microscopy (TMAFM) measurements were carried out with a NanoScope IIIa controller equipped with a Quadrex Electronics extender module (Veeco Metrology Group/Digital Instruments, Santa Barbara, CA).

The images were acquired in ambient conditions and with commercially available non-contact silicon cantilevers whose force constant, resonance frequency, and curvature of the tip radius were nominally 42 N/m, 320 kHz, and ≤ 10 nm, respectively (NCHR, NanoWorld, Switzerland). The effect of the imaging forces on the height of topographic features was examined. The heights of the prion fibrils appeared constant when the intermittent vertical force was smaller than 10 nN which was employed throughout this study. The scan rates were slower than 4 Hz per imaging line (ca. > 2 min per frame). The microscope was housed in a homemade vibration-isolation stage. The samples for TMAFM measurements were prepared by 10-fold dilution of the incubated prion (0.75 mM) with 200-μL acetic acid (w/w 1%). Approximately 10 μL of the prion sample was drop-cast onto freshly cleaved mica for 1 min. The solution was then removed and the mica was dried gently with a stream of $N_2(g)$. The sample was subjected to vacuum dry (~1 h, < 120 mTorr) prior to imaging.

Solid-State NMR Measurements. All NMR experiments were carried out at ^{13}C and ^{1}H frequencies of 75.5 and 300.1 MHz, respectively, on a Bruker DSX300 NMR spectrometer equipped with a commercial 2.5 mm triple-resonance probe. The MAS frequency variation was limited to ± 2 Hz using a commercial pneumatic control unit (Bruker, MAS II). Each fibrillized sample of approximately 6 mg was confined in the middle one-half of the rotor volume using Teflon spacers. Typically, during the cross polarization contact time (1.5 ms), the ^{1}H nutation frequency was set to 50 kHz and that of ^{13}C was ramped through the Hartmann-Hahn matching condition.[1,2] Unless stated otherwise, continuous-wave and XiX[3] proton decouplings (100 kHz) were applied during recoupling periods and the t_2 acquisition, respectively. To reduce the sample heating due to fast MAS spinning, a stream of dry cooling air at –11°C (800 L/h) was used to keep the sample temperature at around 30°C, calibrated by measurements on lead (II) nitrate. ^{13}C NMR chemical shifts were referenced to tetramethylsilane (TMS), using adamantane as the secondary reference standard. ^{15}N NMR chemical shifts were referenced to liquid NH_3, based on the published ratios of ^{13}C and ^{15}N NMR frequencies.[4]

$^{13}C/^{13}C$ chemical shift correlation spectra were measured at an MAS frequency of 25.0 kHz based on the finite-pulse radio frequency-driven recoupling (fpRFDR) technique.[5] During the fpRFDR recoupling periods, the ^{13}C π pulses were 12 μs ($\tau_p/\tau_r = 0.3$). The mixing time was 1.6 ms. $^{15}N/^{13}C$ chemical shift correlation spectra were measured at an MAS frequency of 9.0 kHz, using a frequency-selective $^{15}N–^{13}C$ cross-polarization technique with mixing time of 1.5 ms.[6] Chemical shift and linewidth data were obtained by fitting the cross peaks to a Gaussian using the package NMRPipe.[7]

$^{13}C–^{13}C$ dipolar recoupling measurements were carried out with the constant-time fpRFDR (fpRFDR-CT) technique,[5,8] at an MAS frequency of 20.0 kHz. The ^{13}C π/2 and π pulses were 4 and 15 μs, respectively. The effective dipolar dephasing period was from 0 to 67.2 ms in steps of 4.8 ms. The power level for the ^{13}C π pulse was optimized by maximizing the initial signal. Continuous-wave proton decoupling was 80 kHz during the recoupling period. Total acquisition time for the fpRFDR-CT data was 17 h, using a 4 s recycle delay.

Determination of the backbone torsion ψ angle was performed by correlating the chemical shift anisotropy of the carbonyl carbon and the ^{13}C-^{1}H heteronuclear dipole-dipole interaction of the alpha carbon.[9] Experiments were carried out at an MAS frequency of 25 kHz. The π/2 Gaussian selective pulse was set to 475 μs long and positioned at the aliphatic region. The ^{13}C nutation frequencies were set to 60 and 125 kHz for $R12_5^4$ and for the R-TOBSY pulse block, respectively, as required by the pulse symmetries.[10,11] The R-TOBSY mixing time was set to 7.68 ms, during which no proton decoupling was applied.[12] The Lee-Goldburg (LG) irradiation was achieved by setting the ^{1}H decoupling field and the resonance offset at 81.6 kHz and 57.8 kHz,

respectively, so that the effective nutation frequency was equal to 100 kHz.[13] The duration of the LG irradiation was fixed to three rotor periods. A more detailed description of the method was given elsewhere.[9] Typically, the total acquisition time for each sample was 96 h, using a 3 s recycle delay.

$^{13}C\{^{15}N\}$ rotational echo double resonance (REDOR) measurements were carried out with active rotor synchronization of π pulses on the ^{15}N and ^{13}C channels. The pulse sequence developed by Anderson et al. was employed at an MAS frequency of 8.00 kHz.[14,15] The power level of the ^{15}N π pulses was optimized by maximizing the REDOR dephasing effect. To enhance data reproducibility, the memory buffer for acquisition was manipulated in such a way that the odd- and even-numbered scans were accumulated separately for the REDOR (S) and spin-echo (S_0) signals, respectively. Total acquisition times for the REDOR data were 38 h, using a 4 s recycle delay.

Numerical Analysis of NMR Data. Numerical simulations were carried out using the package SIMPSON (version 1.1.0).[16] The maximum time step over which the Hamiltonian is approximated to be time-independent was set to 1.0 μs. Typically, a powder averaging scheme containing 100 REPULSION angles (α and β)[17] and 18 γ angles was chosen. Relaxation effects were ignored. Simulation parameters were matched to the experimental conditions. Simulations of fpRFDR-CT data were carried out on a linear chain of five equally spaced ^{13}C nuclei, with initial ^{13}C spin polarization on the central spin.

III. Results and Discussion

TMAFM. Panel a of Figure 1 displays a typical AFM image verifying that, after 1-day incubation at 37°C, the peptides $SHPrP_{109–122}$ become fibrils with a length of over 400 nm. The fibrils exhibit a uniform height of 0.9 ± 0.1 nm. This height is consistent with a supramolecular

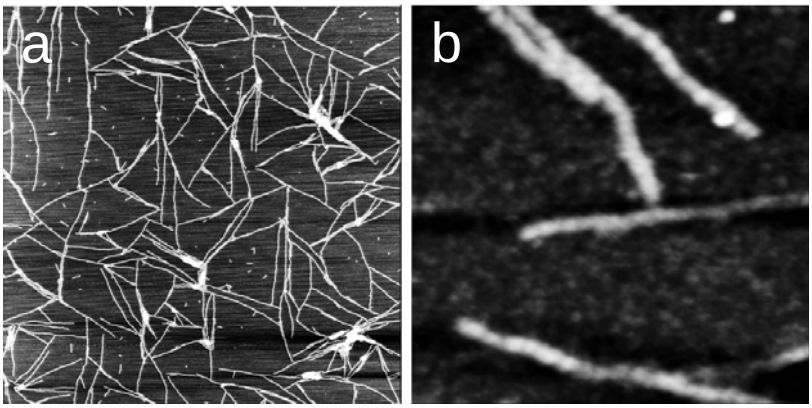

Figure 1. TMAFM images of fibrils on mica in air. Scan size: (a) 2 m x 2 m, (b) 250 nm x 250 nm. The sample was incubated in 37°C for one day.

structural arrangement which comprises the lateral association of two fibrils. From the section profiles along the transversal direction of the fibrils, their widths are found 11.2 ± 1.3 nm which, however, is overestimated due to the finite curvature of the AFM tips. To circumvent this problem, the width is obtained from close-packed fibrils, for example, at the upper portion of Figure 1b. The peak-to-peak distance of the section profile renders a width of ~9 nm. Also revealed in the high-resolution images (Figure 1b) is the bead-like periodicity with the modulation length and depth of 11 nm and 0.24 nm, respectively. Such beaded chains look similar to protofibrils reported in the early stage of Aβ fibril formation.[18,19]

Chemical Shift Data. NMR chemical shifts and linewidth data obtained from the two-dimensional $^{13}C/^{13}C$ and $^{13}C/^{15}N$ chemical shift correlation spectra are summarized in Figures 2 and 3. The data are consistent with a single β-strand conformation for the whole peptide. The full-widths at half maximum ($\Delta\nu_{1/2}$) of the ^{13}C signals arising from the residues in

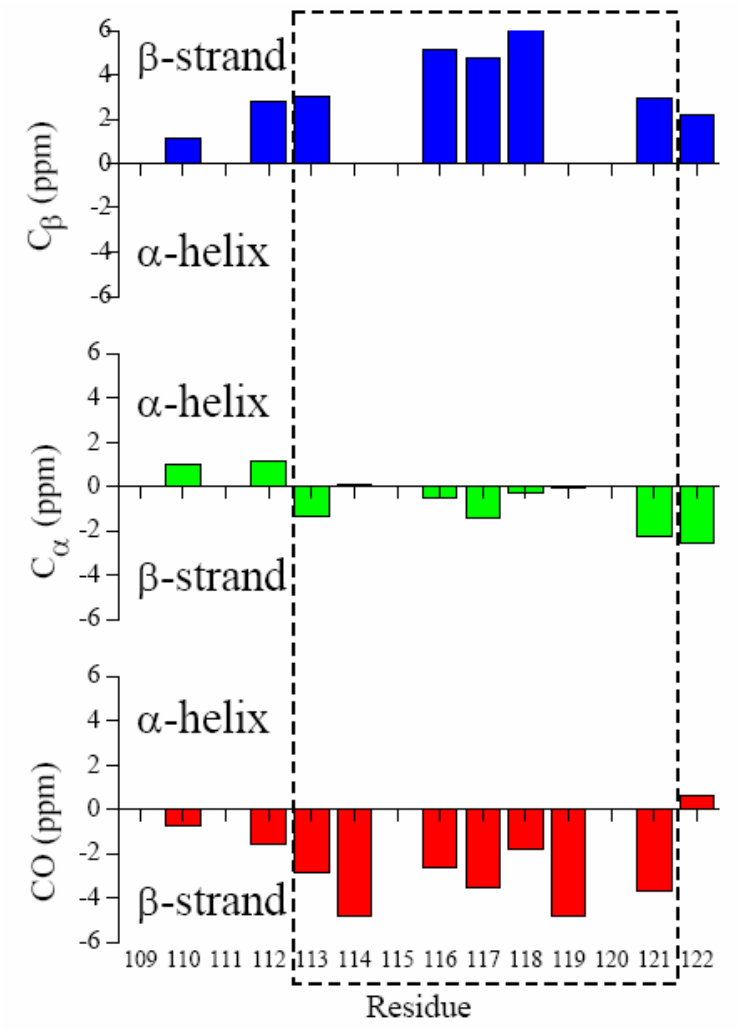

Figure 2. Secondary shifts of selected ^{13}C labeled residues. The ^{13}C chemical shifts of the region highlighted by a dashed rectangular box are consistent with β-strand conformation.

the central peptide region are in the range of 1.6–2.7 ppm, which are characteristic of well-structured fibril samples.[20] In comparison, the $\Delta\nu_{1/2}$ data of the residues K110, M112, and V122 are significantly broader, revealing a considerable structural disorder near the C- and N-termini. It is noteworthy that the residues A116, A117 and A118 have a single sharp peak for each of the CO and C_α signals but have two sharp peaks of comparable intensities for the C_β signal. Because it is not likely that the sidechain of alanine, a methyl group, could adopt two different conformations without affecting the chemical shifts of the CO and C_α, the data imply two different quaternary contacts between the adjacent cross-β layers. We will return to this point below.

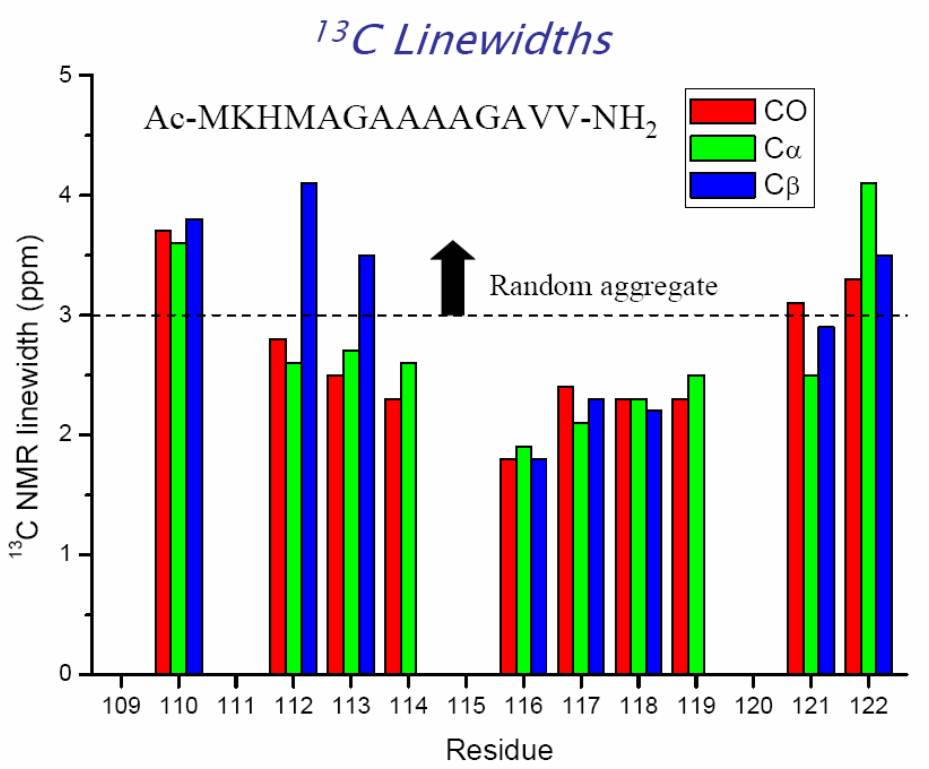

Figure 3. Full widths at half maximum of the ^{13}C NMR signals. The linewidth data indicate that the middle region of the peptide (116-119) is highly ordered.

Determination of Backbone Torsion ψ Angle. The chemical shift data provide a qualitative identification of the backbone torsion angle. To constraint the structural model further, we have developed a quantitative method to directly measure the backbone torsion ψ angle by correlating the chemical shift tensor of the carbonyl carbon and the C_α–H_α dipolar tensor. The results are summarized in the following table:

	M112	A113	A116	A117	A118	V121	V122
ψ	163 ± 9	158 ± 3	155 ± 5	156 ± 3	157 ± 5	151 ± 5	150 ± 5

The data provide a direct experimental proof that each of the peptide in the fibril adopts the β-strand conformation.

Intermolecular ^{13}C–^{13}C Dipolar Recoupling Experiments. The measurements of intermolecular ^{13}C–^{13}C nuclear magnetic dipole–dipole interaction were carried out using the fpRFDR-CT technique as previously applied for Aβ fibrils.[21] The measured fibril sample AAA is

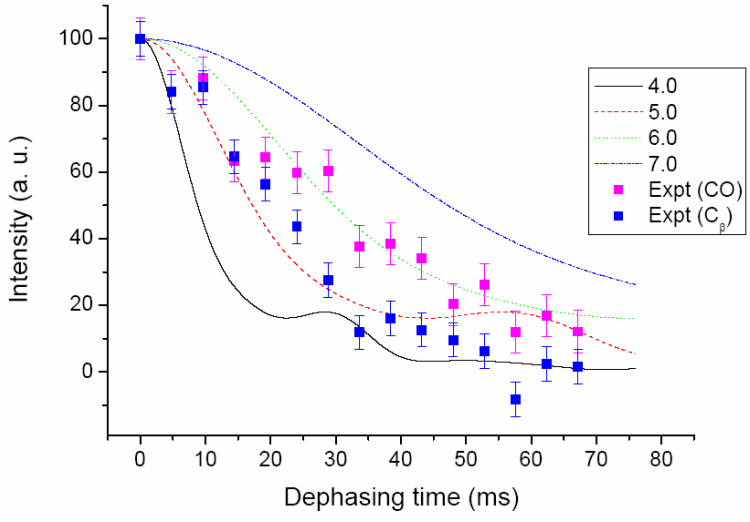

Figure 4. fpRFDR-CT measurements of the AAA sample.

$^{13}C_{\alpha}$-, $^{13}C_{\beta}$- and ^{13}CO-labeled at residues A113, A117, and A120, respectively. Figure 4 shows two sets of fpRFDR-CT data measured by positioning the rf carrier frequency at 28.5 ppm (A117 methyl data) and 168.8 ppm (A120 carbonyl data). Measurement of the A113 methine data was unsuccessful because of the poor signal-to-noise ratio, presumably due to the relatively short transverse spin-spin relaxation time of α-carbons. The A117 methyl data were analyzed by comparison with numerical simulations of a linear chain of six spins with the inter-spin distance ranging from 4 to 7 angstroms, from which the 90% confidence interval of the inter-spin distance lies in the range of 4.91 – 5.63 angstroms. Other data are summarized in the following table:

Spin chain/spin pair	Distance of 90% confidence interval (angstrom)
C_{β}(A117)–C_{β}(A117) spin chain	4.91–5.63
CO(A120)–CO(A120) spin pair	5.78–6.53
CO(G114)–CO(G114) spin pair	6.29–7.06
CO(G119)–CO(G119) spin pair	5.60–6.49

Molecular Dynamics Simulations. A fibril model was created by creating four copies of $SHPrP_{109–122}$ peptides in MOLMOL, which were then arranged according to the motif of anti-parallel cross-β structure. The peptides were aligned in such a way that the residue A117 form a linear chain along the fibril axis. Another similarly created fibril model was positioned in a parallel fashion with respect to the C-terminal of the peptides. We have carried out restrained molecular dynamics and energy minimization simulations, in which all the NMR distance constraints were incorporated:

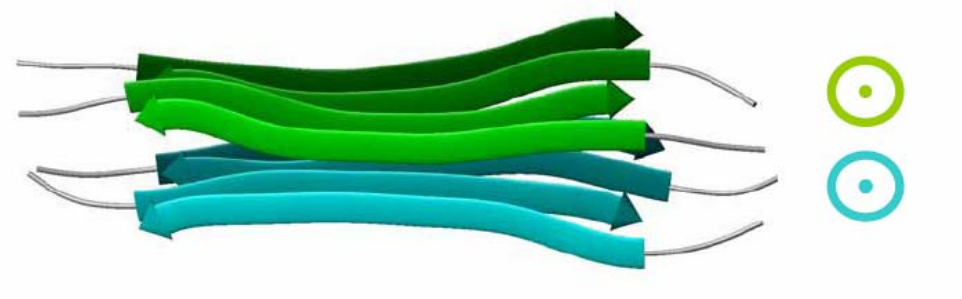

IV. Self Evaluation

In the second year of our project, we have accomplished all our targets. Concerning the solid-state NMR measurements, we have published the following papers:

1. Y Mou, TWT Tsai, JCC Chan*, **2007 APR**, "Determination of the Backbone Torsion Psi Angle by Tensor Correlation of Chemical Shift Anisotropy and Heteronuclear Dipole–Dipole Interaction," *Solid State Nucl. Magn. Reson.*, *31*, 72–81.
2. Y Mou, PH Chen, SW Lee, JCC Chan*, **2007**, "Determination of chemical shift anisotropies of unresolved carbonyl sites by C-alpha detection under magic angle spinning," *J. Magn. Reson.*, in press

These two papers address the NMR technique we developed for the study of filamentous proteins, which provide a technical basis for us to study amyloid fibrils. We are currently writing a manuscript to publish the structural model discussed above in a first-rate journal. We believe our results can provide significant insights into the propagation mechanism of prion proteins. It should be underlined that the structural model reported here is the result of a collaborative effort between the research groups headed by Sheng-Fa Yu, Chun-Hsien Chen, Chun-Yi Lu and

Chun-Chung Chan. Each of the principal investigators has played a decisive role in various aspect of the project. While we have obtained very exciting data on the fibrils formed by $SHPrP_{109–122}$, we are currently investigating the molecular structure of the fibril formed by the fragment $SHPrP_{127–147}$. The fact that $SHPrP_{109–122}$ and $SHPrP_{127–147}$ have very different fibrillization propensity will serve as a valuable model for the study of fibrillization mechanism. In the third year, we will focus on the structural aspect of the fibrillization mechanism.

References

(1) Hediger, S.; Meier, B. H.; Kurur, N. D.; Bodenhausen, G.; Ernst, R. R. *Chem. Phys. Lett.* **1994**, *223*, 283.

(2) Hediger, S.; Meier, B. H.; Ernst, R. R. *Chem. Phys. Lett.* **1995**, *240*, 449.

(3) Detken, A.; Hardy, E. H.; Ernst, M.; Meier, B. H. *Chem. Phys. Lett.* **2002**, *356*, 298.

(4) Wishart, D. S.; Bigam, C. G.; Yao, J.; Abildgaard, F.; Dyson, H. J.; Oldfield, E.; Markley, J. L.; Sykes, B. D. *J. Biomol. NMR* **1995**, *6*, 135.

(5) Ishii, Y. *J. Chem. Phys.* **2001**, *114*, 8473.

(6) Baldus, M.; Petkova, A. T.; Herzfeld, J.; Griffin, R. G. *Mol. Phys.* **1998**, *95*, 1197.

(7) Delaglio, F.; Grzesiek, S.; Vuister, G. W.; Zhu, G.; Pfeifer, J.; Bax, A. *J. Biomol. NMR* **1995**, *6*, 277.

(8) Ishii, Y.; Balbach, J. J.; Tycko, R. *Chem. Phys.* **2001**, *266*, 231.

(9) Mou, Y.; Tsai, T. W. T.; Chan, J. C. C. *Solid State Nucl. Magn. Reson.* **2007**, doi:10.1016/j.ssnmr.2007.01.003.

(10) Levitt, M. H. Symmetry-based pulse sequence in magic-angle spinning solid-state NMR. In *Encyclopedia in Nuclear Magnetic Resonance*, Grant, D. M.; Harris, R. K., Ed. Wiley: Chichester, 2002; Vol. 9, pp 165-196.

(11) Chan, J. C. C.; Brunklaus, G. *Chem. Phys. Lett.* **2001**, *349*, 104.

(12) Mou, Y.; Chao, J. C. H.; Chan, J. C. C. *Solid State Nucl. Magn. Reson.* **2006**, *29*, 278.

(13) Lee, M.; Goldburg, W. I. *Phys. Rev. A* **1965**, *140*, 1261.

(14) Anderson, R. C.; Gullion, T.; Joers, J. M.; Shapiro, M.; Villhauer, E. B.; Weber, H. P. *J. Am. Chem. Soc.* **1995**, *117*, 10546.

(15) Gullion, T.; Schaefer, J. *J. Magn. Reson.* **1989**, *81*, 196.

(16) Bak, M.; Rasmussen, J. T.; Nielsen, N. C. *J. Magn. Reson.* **2000**, *147*, 296.

(17) Bak, M.; Nielsen, N. C. *J. Magn. Reson.* **1997**, *125*, 132.